Malignant transformation of host stromal fibroblasts derived from the bone marrow traced in a dual-color fluorescence xenograft tumor model

XINGLIANG DAI[1], HUA CHEN[2], YANMING CHEN[1], JINDING WU[1], HAIYANG WANG[1], JIA SHI[2], XIFENG FEI[3], ZHIMIN WANG[3], AIDONG WANG[1], JUN DONG[1], QING LAN[1] and QIANG HUANG[1]

[1]Department of Neurosurgery, the Second Affiliated Hospital of Soochow University, Jinchang, Suzhou 215004;
[2]Department of Neurosurgery, the First Affiliated Hospital of Nanjing Medical University, Nanjing, Jiangsu 210029;
[3]Department of Neurosurgery, Suzhou Kowloon Hospital, Shanghai Jiaotong University School of Medicine, Jinchang, Suzhou, 215021, P.R. China

Received June 22, 2015; Accepted August 3, 2015

DOI: 10.3892/or.2015.4281

Abstract. Solid tumors are abnormal tissues containing tumor and non-tumor cells, also known as tumor stromal cells. However, the malignant potential of tumor stromal cells remains largely unknown. The aim of the present study was to investigate the malignant potential of host bone marrow-derived stroma cells in transplanted subcutaneous tumors of the glioma stem/progenitor cells (GSPCs) labeled using the dual-color fluorescent tracer technique. The previously established human glioma stem/progenitor cell line SU3 was transfected with red fluorescence protein (SU3-RFP) and transplanted subcutaneously into green fluorescent protein (GFP) transgenic nude mice and chimeric mice in which GFP was only expressed by bone marrow-derived cells (BMDCs). The xenograft tumors were subcultured *in vitro* and two immortalized GFP-expressing stromal cell lines were cloned from the transplanted tumors. The two cloned cell lines showed an accelerated growth rate, loss of cell contact inhibition, high cloning efficiency, and high DNA content and telocentric (murine) chromosomes with heteroploid characteristics. The tumorigenesis rate (10/10, $1x10^6$) of these host stromal cells was further evidence of malignant transformation. Immunofluorescence assay of the two host cell lines showed that they expressed fibroblast markers such as FAP, S100A4 and α-SMA, as well as mesenchymal cell markers such as CD44 and CD105. In conclusion, bone marrow-derived stromal fibroblasts recruited to tumors have the potential for malignant transformation induced by the tumor microenvironment, which provides new evidence for the role of the stroma in malignant transformation.

Correspondence to: Professor Qing Lan, Department of Neurosurgery, The Second Affiliated Hospital of Soochow University, 1055 Sangxiang Road, Jinchang, Suzhou 215004, P.R. China
E-mail: szlq006@163.com

Key words: malignant transformation, cancer-associated fibroblasts, transgenic green fluorescent nude mice, glioma stem cells

Introduction

Tumors are insular masses of proliferating cancer cells that contain complex tissues of multiple distinct cell types that interact with each other (1). Neoplastic cells recruit and incorporate adjacent or distant healthy host cells, such as bone marrow-derived cells (BMDCs) for support and essential nutrients (2). Neoplastic cells also recruit fibroblasts, mesenchymal cells, macrophages, endothelial cells, pericytes, hematopoietic cells and extracellular matrix (3), all of which together with other components constitute the tumor microenvironment (TME) (1). Tumor host cells exchange cytokines (such as IL-6, GM-CSF and IL-4), extracellular matrix proteins, enzymes and vesicles in distinct sizes, which promote tumor development, progression and metastases (4,5). Nevertheless, how recruited stromal cells respond to the TME as well as tumor cells has constituted a matter of investigation in recent years only and, remains poorly understood.

Fibroblasts are present in various tumors. These fibroblasts are termed cancer-associated fibroblasts (CAFs) and, in many cases, constitute the majority of the cell population of the tumor stroma (1). CAF includes two distinct cell types: i) one cell type is similar to fibroblasts and forms the structural supporting epithelial tissues, and ii) the other type, myofibroblasts, has biological roles and properties that are markedly different from those of tissue-derived fibroblasts. Myofibroblasts are identified by their expression of α-smooth muscle actin (α-SMA). CAFs have several origins. While some studies showed that the main progenitor of CAFs appears to be the local residing fibroblasts (6), other authors suggest that CAFs originate from the bone marrow and are derived from mesenchymal stem cells (MSCs) (7-11). Bone marrow-derived MSCs also comprise a large portion of the tumor stroma, and can differentiate into a variety of other cell types, such as fibroblasts and endothelial cells. Irrespective of their origin, CAFs promote tumor cell growth, invasion and metastasis, and are therefore well recognized as an important prognostic indicator in various types of carcinomas (4-13). Furthermore, CAFs, but not normal fibroblasts, can stimulate prostatic epithelial proliferation, immortalization and malignant transformation (14,15), even without apparent mutations in the epithelial cells themselves (16,17). Early evidence has indicated that CAFs are different from normal fibroblasts with regard to their structure, autocrine growth factor signaling pathway, proliferation and migratory behavior (18-20). However, genetic alteration of tumor stromal cells (CAFs) under the influence of the TME, which is known to cause tumor development and progression, has not received much attention. Although several studies have demonstrated the association of certain CAF mutations with carcinomas (21-23), these mutations were only associated with the initiation of epithelial cell carcinomas (19,24) and their role in their own malignant transformation remains to be elucidated. Stromal cells recruited to the TME are termed 'non-tumor' cells and are known to play a role in tumor progression or suppression. These stromal cells are considered normal and never undergo malignant transformation (2,25-27). However, the malignant transformation of the tumor stromal cells, particularly CAFs and their origin, MSCs, *in vitro* and *in vivo* has been previously reported (28-34). Therefore, this remains a controversial topic that requires further investigation.

The fluorescent protein gene tracer technique is useful for visualization of the TME. The use of transgenic nude mice with ubiquitous fluorescent protein expression as hosts for human tumors makes it convenient to observe the interactions between tumor and host cells (35-38). Suetsugu *et al* (39) successively passaged human tumor specimens in transgenic nude mice ubiquitously expressing red fluorescent protein (RFP), green fluorescent protein (GFP) and cyan fluorescent protein (CFP). They identified that stromal components, such as CAFs, tumor-associated macrophages (TAMs) and blood vessels expressing RFP, GFP and CFP, coexist in the transplanted tumor and demonstrated its serial transplantability (39). The transplantability of tumor-associated stromal cells was also previously demonstrated by other authors (40). However, the outcome of these stromal cells is crucial. In the present study, the dual-color fluorescent protein tracer technique in a mouse model with RFP-expressing tumor cells and GFP-expressing nude mice was used to observe the malignant transformation of the host derived GFP-expressing stromal cells. It was confirmed that these transformed stromal cells were derived from the bone marrow. Previously, we reported the host macrophage carcinomas of abdominal xenograft tumors (41). In the present study, we also reported the malignant transformation of bone marrow-derived stromal fibroblasts via the transgenic nude mouse model with ubiquitous GFP expression and BMDCs expressing GFP only.

Materials and methods

Cell culture and transfection with the RFP gene. The highly invasive glioma stem cell (GSC) line SU3 was previously established in our laboratory (42,43). SU3 cells were transfected with the *RFP* gene using a pLenO-RIP plasmid vector, which carries a puromycin-resistant gene according to the manufacturer's instructions (Invabio Biotechnology, Shanghai, China). RFP-transfected SU3 cells (SU3-RFP) cells were amplified in Dulbecco's modified Eagle's medium (DMEM) containing 10% fetal bovine serum (FBS) (both from HyClone, Logan, UT, USA), 100 IU/ml penicillin, 100 μg/ml streptomycin and 10 μg/ml puromycin to select the transduced cells. SU3-RFP stem/progenitor cells were cultured in stem cell medium, i.e., DMEM/F12 (Gibco, Carlsbad, CA, USA), containing 20 ng/ml basic fibroblast growth factor (bFGF; PeproTech, Rocky Hill, NJ, USA), 20 ng/ml epidermal growth factor (EGF; Invitrogen Life Technologies, Carlsbad, CA, USA), B27 supplement (50X), 2 mmol/l L-glutamine (100X), MEM vitamin solution (100X) and 100 mM sodium pyruvate (100X) (all from Gibco). Immunohistochemical staining with monoclonal antibodies against CD133 (Miltenyi, Bergisch Gladbach, Germany), nestin (BD Biosciences, San Jose, CA, USA), GFAP (Santa Cruz Biotechnology, Inc., Santa Cruz, CA, USA) and β-tubulin-III (BD Biosciences) was performed to detect the expression of the markers and determine the cell type of the differentiated cells.

Transgenic GFP nude and chimeric mice. Transgenic C57BL/6-GFP and BALB/c athymic nude (nu/nu) mice were purchased from the Model Animal Center of Nanjing University (Nanjing, China). C57BL/6-GFP mice expressed GFP under the control of the CAG promoter (CMV-IE enhancer chicken β-actin promoter and rabbit β-globin genomic DNA) (36,44). Findings of a previous study (36) revealed that GFP nude mice were generated by crossing BALB/c nude mice with C57BL/6-GFP mice. Continuous back-crossing for 10 generations was then performed to purify the background to BALB/c. To establish chimeric mice, the bone marrow of BALB/c athymic nude (nu/nu) mice was subjected to 6 Gy of radiation to destroy the bone marrow, which was then rebuilt from GFP nude mice. Only bone marrow-derived cells expressed GFP in this chimeric mouse model. The animals were maintained under the specific pathogen-free environment at the Animal Center of Soochow University. The animal studies were conducted in accordance with the approved facilities of the Chinese Experimental Animal.

Establishment of the xenograft tumor and subculturing. Six-week-old GFP nude mice received an injection of 1×10^6 SU3-RFP cells in a total volume of 50 μl in the armpit of the right forelimb via a Hamilton syringe. Whole-body images of the tumor-bearing mice were obtained using the In Vivo Imaging System FX Pro (Kodak, Rochester, NY, USA) under excitation at 470 and 535 nm after induction of anesthesia. The mice were then sacrificed and a section of the transplanted tumor tissues was fixed with 4% paraformaldehyde, dehydrated in 20% and then 30% sugar, and used to make 5-μm frozen sections. The sections were stained with hematoxylin and eosin (H&E) or observed directly under a fluorescence microscope after staining with 4',6-diamino-2-phenylindole (DAPI; KeyGen, Nanjing, China). Confocal laser-scanning microscopy was performed to monitor the mutual interactions between tumor and host cells. The other section of the tissues was harvested and washed with phosphate-buffered saline (PBS) containing penicillin and streptomycin, three times. The section was then minced with fine scissors into small fragments, and cultured in culture medium containing 10%

FBS. The medium was replaced with fresh culture medium the following day. Normal cell culture conditions were maintained for the subsequent days.

Identification and cloning of the GFP-positive cells. After several passages, the GFP-positive cells multiplied persistently until a stable percentage of the total cells was reached. Adherent cells were digested in a single-cell suspension using the Accutase Cell Dissociation Reagent (Gibco), and sorted using a cell sorter (MoFlo XDP; Beckman Coulter, USA) into three or four groups: cells emitting red and green fluorescence, both red and green fluorescence, and/or cells without fluorescence. Cells emitting green fluorescence were collected and cultured in fresh medium containing 10% FBS. A single cell was obtained using a capillary pipette and cultured in 96-well plates.

Growth characteristics of the GFP-positive cells

Proliferation assay. Cell proliferation was evaluated using soft agar colony assay and Cell Counting Kit-8 (CCK-8; Dojindo Laboratories, Mashikimachi, Kamimashiki Gun, Kumamoto, Japan) according to the manufacturer's instructions. For the CCK-8 assay, the cells were seeded at 1×10^3 cells/well in 96-well plates and cultured in 100 μl medium. SU3-RFP, NIH-3T3 and blank control (only medium and CCK-8 solution) were set at the same time. CCK-8 solution (10 μl/well) was added and then incubated at 37˚C for 2 h. The optical density (OD) at 450 nm was recorded by a microplate teader (Tecan Infinite 200 PRO; Salzburg, Austria). Each experiment was performed three times in 6-well plates.

Cell cycle assay. For the cell cycle assay, the cells were harvested in the logarithmic phase, washed with ice-cold PBS, and fixed with 70% ethanol and stored at -20˚C for at least 24 h. Prior to analysis, the fixed cells were centrifuged for 10 min at 2,000 g and resuspended in PBS incubated with 0.5 mg/ml RNase A (Sigma R-4875; St. Louis, MO, USA) and 25 μg/ml propidium iodide (PI; KeyGen Biotech, Nanjing, China) for 30 min at room temperature in the dark. SU3-RFP and mouse peripheral blood lymphocytes (LYM) were used as the control. The cells were counted using flow cytometry (Cytomics FC 500; Beckman Coulter) and analyzed using CXP software (Beckman Coulter).

Soft agar colony assay. For the soft agar colony assay, the cells (1×10^3/well) were suspended in 2X DMEM containing 20% FBS, mixed with the same volume of 0.7% low-melting agarose (Lonza, Allendale, NJ, USA), and seeded over a layer of 0.5% agar in a 6-well plate. After 15 days of incubation, colonies with >20 cells were counted and photographed using an inverted microscope (Olympus CKX31; Tokyo, Japan).

Genetic characteristics of the GFP-positive cells

RT-PCR, karyotype analysis and DNA content. GFP expression of the transformed cells was detected using PCR as previously described (41). GFP transgenic mouse tail was used as the positive control and the mouse NIH-3T3 cell line was used as the negative control, and specific human and mouse primer pairs were used to identify the cell species. Primers of the *GFP* gene were: 5'-GCCACAAGTTCAGCGTGTCCG and 5'-GTTGGGGTCTTTGCTCAGGGCG (566 bp); RFP, 5'-AGGTTCTTAGCGGGTTTCTTG and 5'-CTTCCCTGA GGGCTTCACAT (312 bp); human-specific β-action, 5'-ACA TCCGCAAAGACCTATAC and 5'-GCCATGCCAATCTCA TCTTG (346 bp); mouse-specific β-action, 5'-CTTTGCAGC TCCTTCGTTG and 5'-TGGTAACAATGCCATGTTCA (278 bp). Karyotyping of these cells was performed as previously described (45). Cell DNA content and the cell cycle were analyzed using flow cytometry. For the DNA content assay, the cell density of the sample and control cells after staining with PI were adjusted until they were the same and sample flow was strictly controlled. Proper maintenance and careful adjustment of the instrument were ensured prior to analysis. The mouse blood lymphocytes from the same strain were extracted as the control cells.

Immunofluorescence analysis. The immunofluorescence analysis was performed as previously described (42). Briefly, frozen sections were produced as described earlier. Tissue sections were stained with antibodies against α-SMA (ab5694, 1:100; Abcam, Cambridge, USA), S100A4 (ab27957, 1:100), FAP-α (ab53066), CD44 (ab25340, 1:200), CD105 (ab107595) and Ki67 (ab16667, ab15580, 1:50). Cy3-labeled goat anti-rabbit IgG and Alexa Fluor 488-labeled goat anti-rabbit IgG (Beyotime, Shanghai, China) were used as secondary antibodies. Expression of the aforementioned cell surface markers was detected with a fluorescence microscope (Olympus IX51; Tokyo, Japan), and images were captured and merged using the software provided.

Tumorigenicity in nude mice. To verify the tumorigenicity of the GFP-positive cells, BALB/c nude mice (n=10) and normal mice (n=10) aged 5 weeks, were injected with 1×10^7 and 1×10^6 GFP-positive cells in the armpit of the right forelimb, respectively. Tumor-bearing mice were sacrificed 25 days later, and the transplanted tumor tissues were sectioned and stained with H&E and DAPI. Images were captured and merged using a phase-contrast and a fluorescence microscope.

Statistical analysis. Each experiment was performed as least three times, and data are presented as the mean ± SD where applicable. Differences were evaluated using the Student's t-tests for two-group comparisons. $P<0.05$ was considered to indicate a statistically significant result. Each group was analyzed using the GraphPad Prism 5.0 software.

Results

RFP-expressing SU3 cell line. The SU3-RFP showed almost 100% expression of RFP (Fig. 1A and D). The *in vitro* growth characteristics of the stem and adherent cells were similar to those of the SU3 cells without the RFP vector (Fig. 1B, C and E). As with the SU3 cell lines previously reported (43), the SU3-RFP cells also showed a high expression of CD133 and nestin in the stem cells when cultured in stem cell medium (Fig. 1F and G). GFAP- and β-tubulin III-positive cells were observed with 10% FBS supplementation (Fig. 1H and I).

GFP-positive host stroma cells. As previously reported (44), transgenic EGFP nude mice ubiquitously expressed green

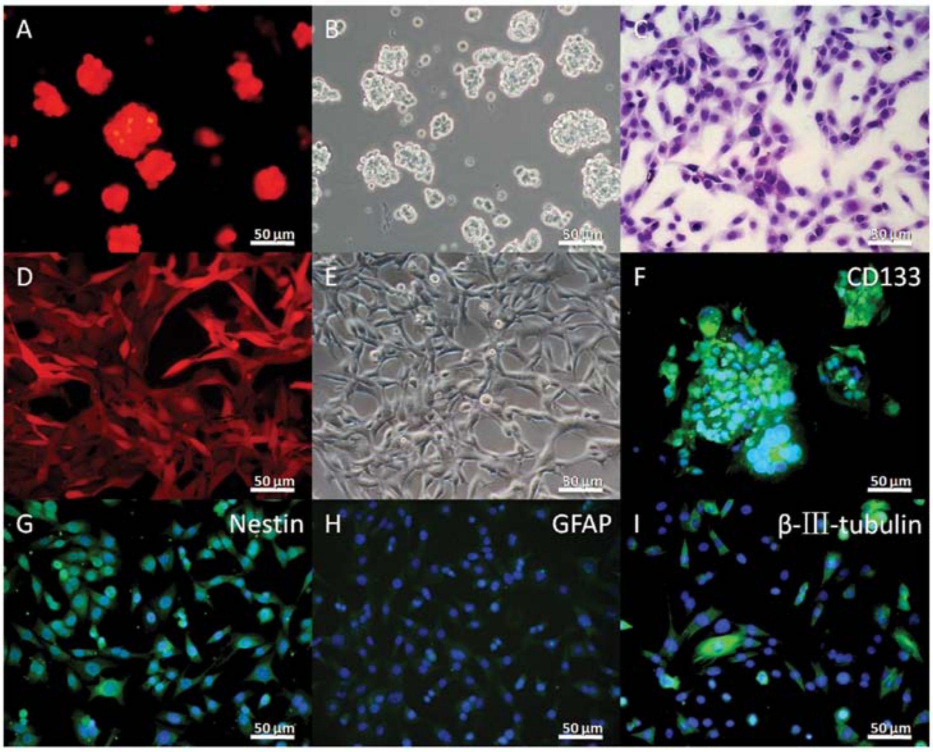

Figure 1. Characteristics of the glioma stem cell line SU3 transfected with the red fluorescence protein gene. (A) SU3-RFP cell spheres under the fluorescence microscope. (B) SU3-RFP cell spheres under the phase-contrast microscope. (C) H&E-stained SU3-RFP cells. (D) Adherent culture of SU3-RFP cells under the fluorescence microscope. (E) adherent culture of SU3-RFP cells under the phase-contrast microscope. (F) Expression of CD133 in the SU3-RFP cell spheres. (G) Expression of nestin in the SU3-RFP cells prior to differentiation. (H) expression of GFAP in the SU3-RFP cells after differentiation. and (I) Expression of β-III-tubulin in the SU3-RFP cells after differentiation. Scale bar, 50 μm.

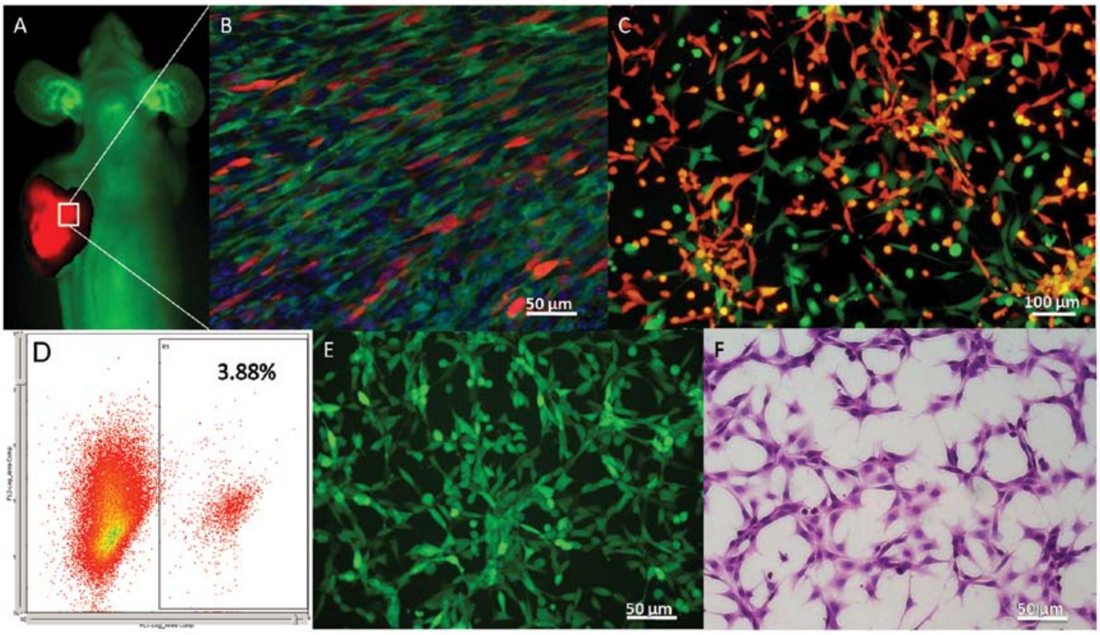

Figure 2. Tumor transplantation in the transgenic nude mice. (A) SU3-RFP xenograft tumor in the GFP nude mice. (B) Frozen sections of the xenograft tumor under a confocal microscope. stained with DAPI (blue nucleus). (C) Primary subculturing. (D) GFP-positive cells sorted by flow cytometry: 3.88% GFP-positive cells were obtained. (E) Sorted GFP-positive cells under the fluorescence microscope. (F) H&E-stained GFP-positive cells: the cells are spindle-like or polygonal in shape. have a large and hyperchromatic nucleus and are obviously heterogeneous. Scale bars, B, C, E and F, 50 μm.

fluorescence, except for the hair and red blood cells under blue light (Fig. 2A). The transplanted tumor showed bright red fluorescence under excitation with green light (Fig. 2A). On the frozen DAPI-stained sections, GFP-positive host stromal cells showed marked proliferation and accounted for a large proportion of the total cells (Fig. 2B). After subculturing, the

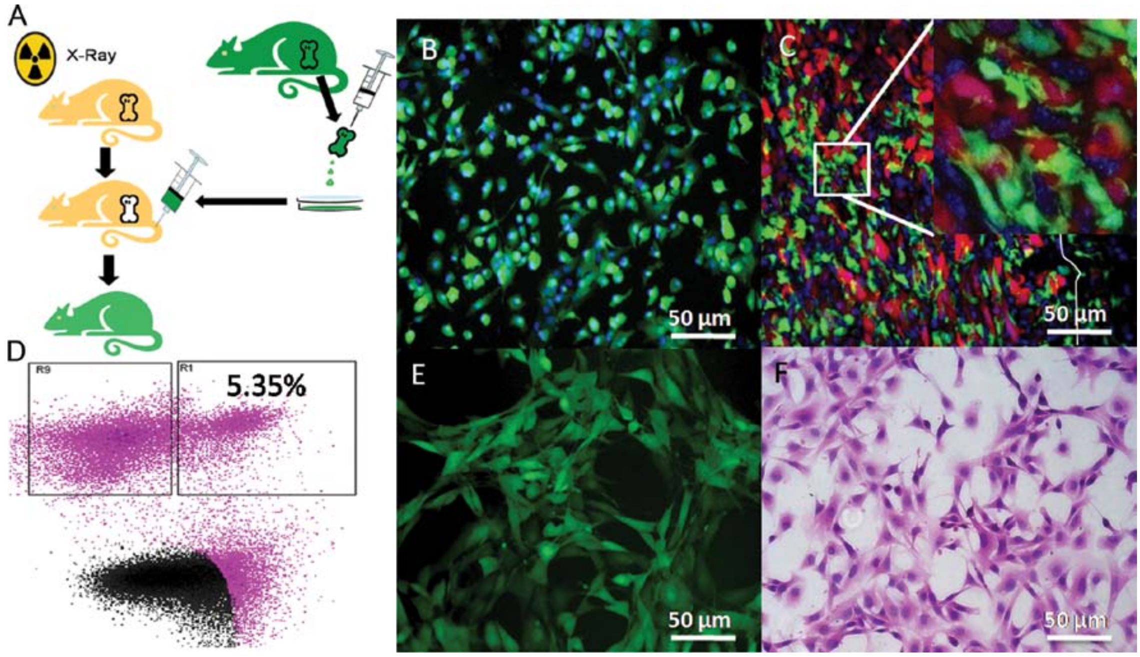

Figure 3. Chimeric mice with bone marrow-derived cell expressing GFP and the tumor model. (A) Schema of chimeric mice with only bone marrow-derived cell expressing GFP. (B) DAPI-stained cells flushed from the bone marrow (blue nucleus). (C) Xenograft tumor tissue under a confocal microscope: the SU3-RFP cells are stained red; the host bone marrow-recruited cells, green; the nucleus, blue (DAPI); and the white smooth curve shows the tumor boundary. (D) GFP-positive cells were sorted by flow cytometry: 5.35% GFP-positive cells were obtained. (E) Sorted GFP-positive cells under the fluorescence microscope. (F) H&E-stained GFP-positive cells, observed as polygonal cells with a large and hyperchromatic nucleus, and obvious heterogeneity. Scale bar, B, C, E and F, 50 μm.

RFP-positive SU3RFP and GFP-positive host stromal cells were easily distinguished under the fluorescent microscope (Fig. 2C), and the latter accounted for 3.88% of the total cells in the flow cytometric analysis (Fig. 2D), less than the proportion of transplanted tumor tissues. GFP-positive host stromal cells were sorted by flow cytometry and termed SU3-RFP-induced host subcutaneous transformed cells (ihSTCs), which were maintained in continual cultures, similar to immortalized cells (Fig. 2E). These spindle-shaped cells, which showed strong nuclear staining and had an unlimited capacity for proliferation, had similar characteristics to malignant tumor cells (Fig. 2F).

In the chimeric mice, the bone marrow system was rebuilt (Fig. 3A), with almost all the bone marrow-derived cells expressing GFP (Fig. 3B). In the xenograft tumors, interactions between SU3-RFP cells and bone marrow-derived GFP-positive cells were clearly observed under a confocal laser-scanning microscope (Fig. 3C). The GFP-positive cells were sorted by flow cytometry and accounted for 5.35% of the total cells (Fig. 3D), with their growth characteristics being similar to ihSTCs *in vitro* (Fig. 3E and F). The cells were termed SU3-RFP-induced host subcutaneous transformed, bone marrow-derived cells (ihSTBMCs).

Growth characteristics of ihSTCs and ihSTBMCs. In the primary cultured cells, RFP-expressing tumors cells, GFP-expressing host cells, and the small number of GFP-RFP co-expressing cells were easily distinguishable. After short-term subculturing, the cells were digested and sorted using a flow cytometer. The sorted GFP-expressing cells were spindle-like, polygonal or squamous and showed loss of cell contact inhibition under the fluorescence and phase-contrast microscope with H&E staining (Figs. 2F and 3F).

The CCK-8 assay showed that ihSTCs and ihSTBMCs grew rapidly, faster than the SU3-RFP and NIH-3T3 cells (Fig. 4A). This result confirmed that the proliferative abilities of the ihSTCs and ihSTBMCs were higher than those of the original tumor cells.

Results of the cell cycle assay showed that a markedly higher number of ihSTCs and ihSTBMCs were in the S phase (Fig. 4B): 42.33% (Fig. 4D) and 34.91% (Fig. 4E), respectively, in the S phase, higher than the number of SU3-RFP (16.06%, Fig. 4F) and LYM (0.44%, Fig. 4G) cells. Thus, ihSTCs and ihSTBMCs showed an abnormally high DNA synthesis capacity, much higher than that of the SU3-RFP cells ($P<0.0001$).

The agar colony assay showed that the colony formation of ihSTCs (47.37‰) and ihSTBMCs (39.38‰) was significantly enhanced compared to the SU3RFP (10.75‰) and NIH3T3 (0‰) cells (Fig. 4C and H-K) ($P<0.0001$).

Murine origin of ihSTCs and ihSTBMCs. Under the fluorescent microscope, ihSTCs and ihSTBMCs emitted green fluorescence, which proved that the cell lines were host-derived (Figs. 2E and 3E). The origin of the two cell lines was also identified by mRNA analysis using mouse- and human-specific primers. Mouse β-actin was amplified but human β-actin was not amplified in ihSTCs and ihSTBMCs (Fig. 5A). Moreover, the *GFP* gene was expressed in ihSTCs and ihSTBMCs, as well as the control GFP mouse tail, but not in the SU3-RFP or NIH-3T3 cells (Fig. 5A). Karyotype analysis also proved that the chromosomes of the two cell lines were telocentric (Fig. 5C and D), which is characteristic of all

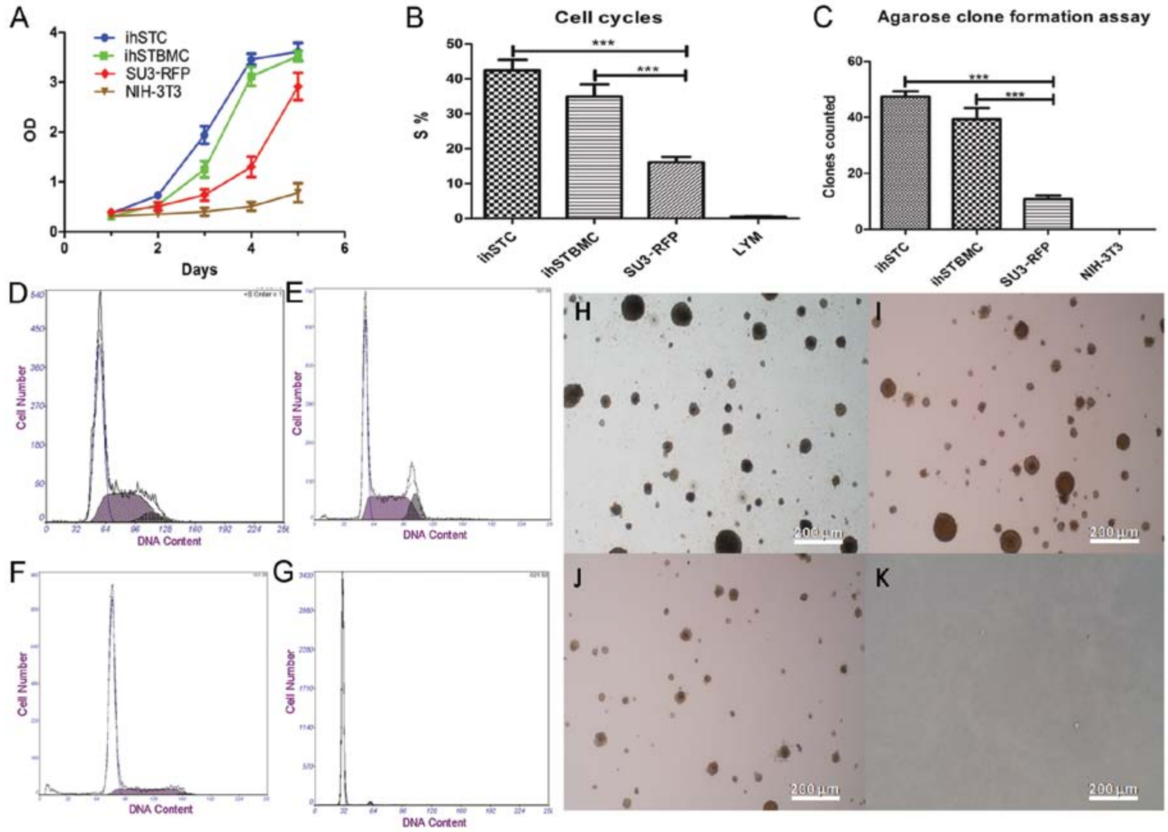

Figure 4. *In vitro* growth characteristics of ihSTCs and ihSTBMCs. (A) Proliferation curve of ihSTCs and ihSTBMCs, SU3-RFP cells and mouse embryonic fibroblast cell NIH-3T3 (control). (B and D-G) Cell cycles of ihSTCs and ihSTBMCs, SU3-RFP and NIH-3T3 cells (control); the S-phase cell fractions of ihSTCs and ihSTBMCs, SU-3RFP and NIH-3T3 cells are 42.33% (D), 34.91% (E), 16.06% (F) and 0.44% (G), respectively. (C and H-K) According to the double-layer agarose clone formation test for cell proliferation ability, the colony-forming efficiency of ihSTCs and ihSTBMCs, SU3-RFP and NIH-3T3 cells was 47.37‰ (H), 39.38‰ (I), 10.75‰ (J) and 0‰ (K), respectively. (H-K) Scale bar, 50 μm.

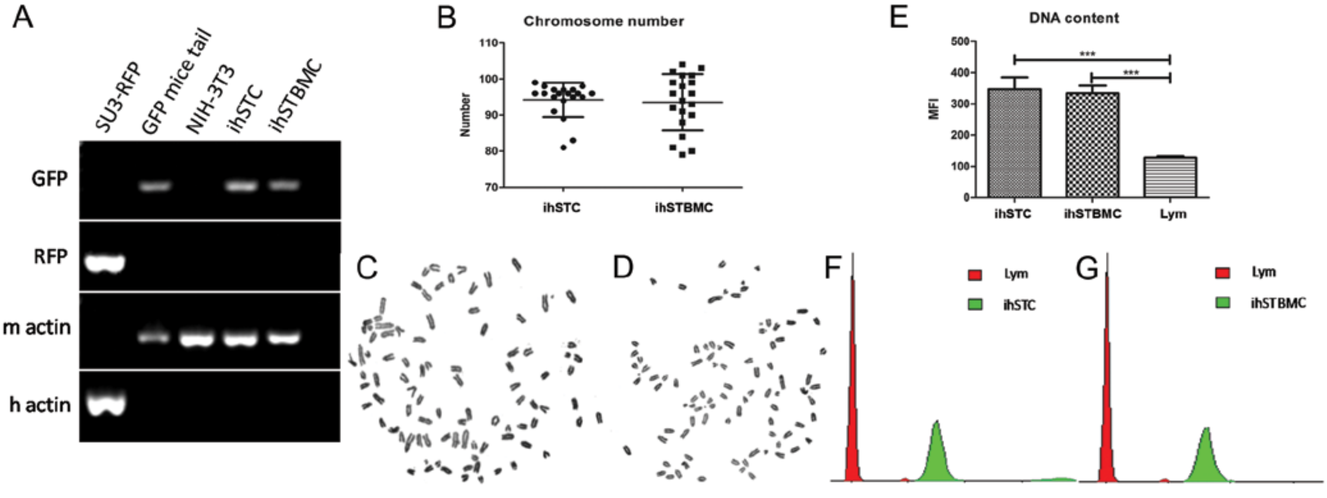

Figure 5. Murine origin of ihSTCs and ihSTBMCs. (A) RT-PCR analysis shows that GFP and mouse-specific β-actin (m actin) were expressed in ihSTCs and ihSTBMCs, but RFP and human-specific β-actin (h actin) were not expressed. The mouse tail tissue and NIH-3T3 cells were used as the control. (B-D) Karyotype analysis shows that only telocentric chromosomes were observed in ihSTCs and ihSTBMCs. The two cells had a heteroploid chromosome with the average chromosome number being 94.25±4.66 (n=20) and 93.55±7.65 (n=20), respectively; (E-G) DNA content of ihSTCs and ihSTBMCs showing that the MFI was 2.71- and 2.61-fold higher than that in the mouse peripheral blood lymphocytes, respectively.

mouse chromosomes. Additionally, the average number of chromosomes of ihSTCs and ihSTBMCs was 94.25±4.66 (n=20) and 93.55±7.65 (n=20), respectively (Fig. 5B-D), which shows the pentaploid characteristics of these cells. The DNA content assay further validated the results of the karyotype analysis, showing that the mean fluorescence intensity

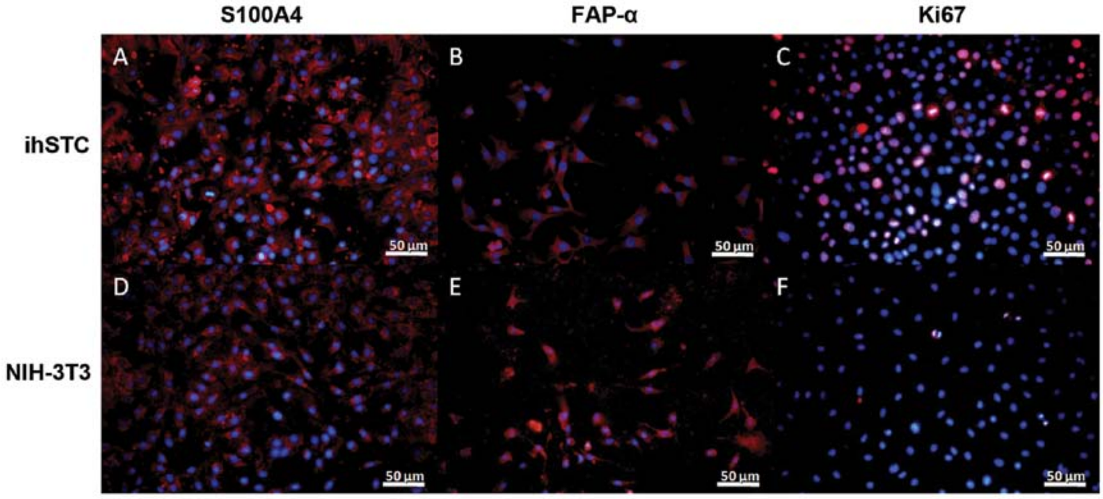

Figure 6. Biomarkers of ihSTCs by immunofluorescence assay. (A) High expression of the fibroblast marker S100A4. (B) High expression of the fibroblast marker FAP-α. (C) High proliferation activity was observed, according to the expression of Ki-67. (D-F) NIH-3T3 was used as the control for S100A4, FAP-α and Ki-67. The cells are stained with DAPI (blue nucleus). (A-F) Scale bar, 50 µm.

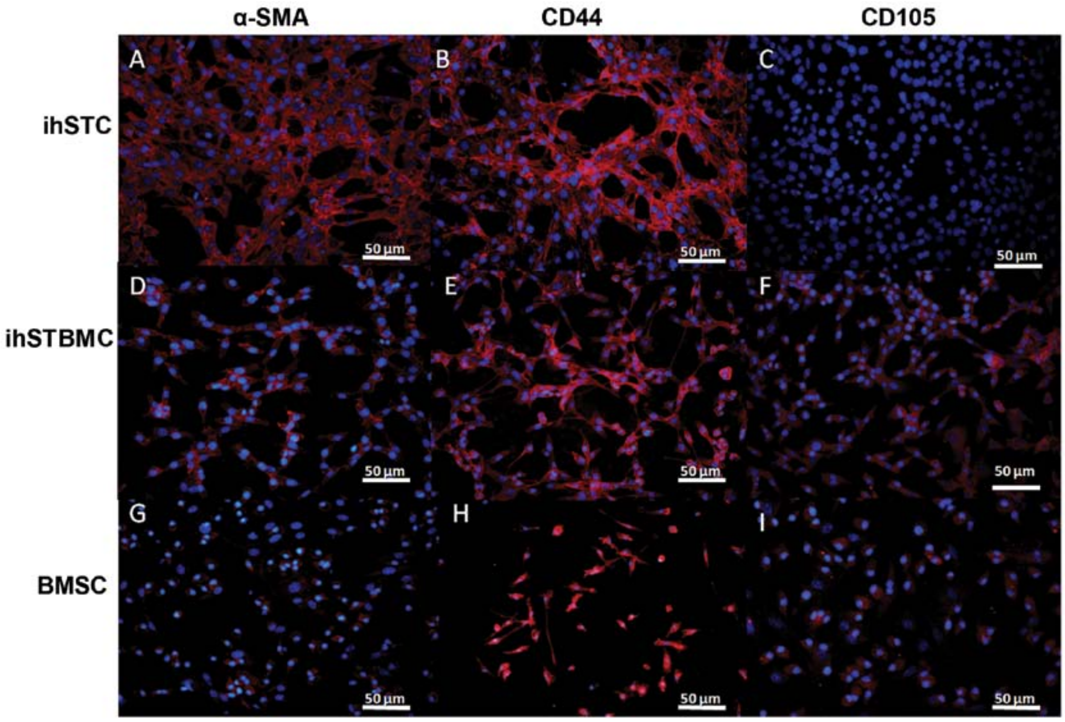

Figure 7. Biomarkers of ihSTBMCs and ihSTCs by immunofluorescence assay. (A-C) High expression of the fibroblast marker α-SMA and the mesenchymal cell marker CD44 was observed in ihSTCs, but the expression of the mesenchymal cell marker CD105 was not observed. (D-F) High expression of the mesenchymal cell markers CD44 and CD105 and the fibroblast marker α-SMA was observed in ihSTBMCs. (G-I) BMSC was used as the control for α-SMA: (G) CD44 (H) and CD105 (I). The cells are stained with DAPI (blue nucleus); (A-I) Scale bar, 50 µm.

(MFI) of ihSTCs and ihSTBMCs was 2.71- and 2.61-fold (Fig. 5E and F, green peaks) that of the mouse lymphocytes, respectively (Fig. 5E and F, red peaks).

The immunofluorescence assay showed that ihSTCs were not only positive for S100A4 (Fig. 6A), FAP-α (Fig. 6B) and α-SMA (Fig. 7A), but also for CD44 (Fig. 7B). Additinoally, ihSTBMCs were positive for CD44 and CD105, as well α-SMA. However, the two cell types were negative for the glioma stem cell markers CD133, nestin, GFAP and β-tubulin III (data not shown). Ki-67 was used as a marker of cell proliferation. S100A4, FAP-α and α-SMA are known as biomarkers of activated fibroblasts, and CD44 and CD105 are common mesenchymal stromal cell markers. Based on these findings and the GFP expression in these cells, ihSTCs and ihSTBMCs appear to be the source of rapidly proliferating host-derived fibroblasts and mesenchymal cells, respectively. Furthermore, transformed fibroblasts may originate from bone marrow-derived mesenchymal stem cells.

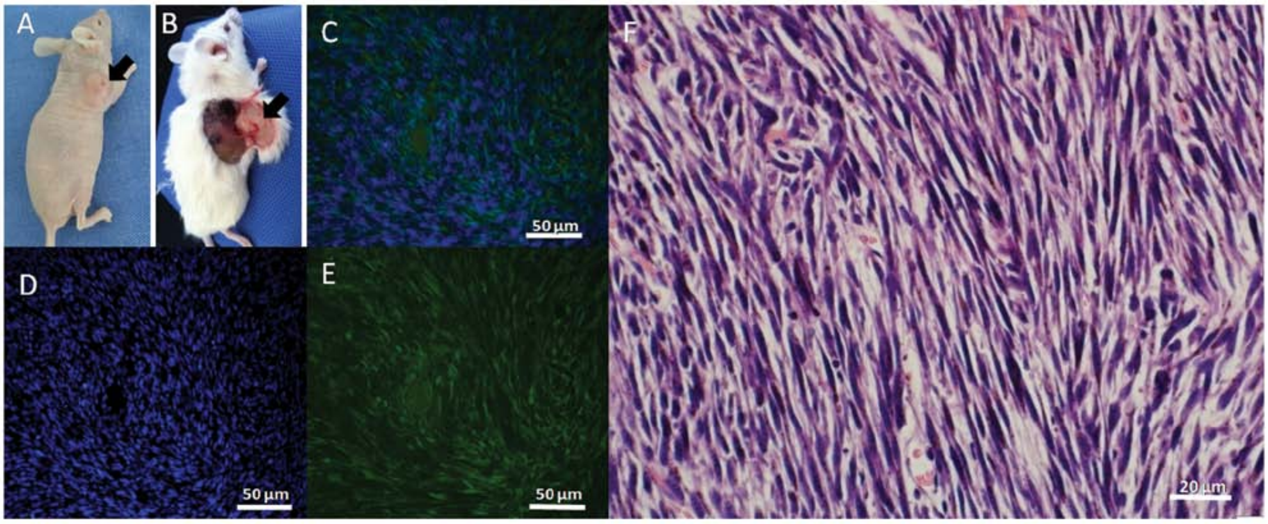

Figure 8. Tumorigenicity in immunosuppression and normal mice. (A) Tumorigenicity of ihSTCs in BALB/c nude mice. (B) Tumorigenicity of ihSTBMCs in normal BALB/c mice. (C-E) Transplanted tumor tissue showing GFP expression, stained with DAPI (blue nucleus). (F) H&E staining of the transplanted tumor showing fibrosarcoma-like changes. (C-E) Scale bar, 50 μm. (F) 20 μm.

Enhanced tumorigenicity in normal and immunosuppressed mice. The two GFP-positive cell lines established showed 100% tumorigenicity (n=10) in nude mice (Fig. 8A), 100% tumorigenicity in normal mice (5/5) at a dose of $1x10^7$ cells/mice and 40% tumorigenicity (2/5) at a dose of $1x10^6$ GFP-positive cells/mouse (Fig. 8B). However, the tumorigenicity of SU3-RFP was only 20% (1/5) in normal mice at a dose of $1x10^7$ cells and 0% (0/5) at a dose of $1x10^6$ cells. These results confirmed that the tumorigenicity of the two GFP-positive cell lines derived from the host mice was stronger than that of the human glioma stem cell line SU3-RFP. Frozen DAPI-stained sections showed that the transplanted tumor tissue was positive for GFP (Fig. 8C-E) and showed fibrosarcoma-like changes with H&E staining (Fig. 8F).

Discussion

The use of fluorescent proteins for imaging the TME by color-coded cancer and stromal cells is highly useful (46), as it provides for non-invasive, dynamic and real-time visualization. We, as well as other investigators, have cultivated GFP athymic nude mice by crossing C57BL/6J-GFP mice with BALB/c nude mice (35-37). The transgenic GFP nude mice are crucial for studying tumor-host interactions. Suetsugu *et al* ((47) demonstrated that GFP-expressing host CAFs are recruited by the host tumor and proliferate, based on fluorescence imaging and suggested the important role of these cells in tumor progression. Previous findings have also shown that CAFs within tumors are derived from bone marrow-derived mesenchymal stem cells (8,48). To determine the role of BMDCS, in the present study, we established a chimeric mouse model in which only the BMDCs expressed GFP. First, we destroyed the bone marrow system of BALB/c nude mice, and then we replaced it with whole bone marrow cells of GFP nude mice via tail vein injection. The BMDCs of these chimeric mice eventually expressed GFP. In the frozen tumor sections, a large number of bone marrow-derived GFP-expressing cells were found to extensively accumulate in the tumor area. However, almost none of the GFP cells accumulated in the adjacent non-tumor area in nude mice. Therefore, this mouse model seems ideal for studying the interactions between tumor cells and BMDCs.

Using this transgenic GFP nude mouse model, in the present study, we cloned a host-derived cell line expressing GFP from the subcutaneous transplantation tumor, and we demonstrated that it was a fibroblast cell line positive for the characteristic biomarkers. The application of the chimeric model also proved that some of the tumor stroma fibroblasts, if not all, were recruited from the bone marrow. To confirm the murine origin of the GFP-expressing cells, mouse-specific mRNA level and karyotype analyses were performed. Only mouse-specific β-actin was amplified and telocentric chromosomes were observed. Based on this evidence, it appears that the two GFP cell lines were derived from the host mouse. *De novo* expression of α-SMA is the most commonly used marker for CAFs, while other widely used CAF markers are fibroblast-specific protein 1 (FSP1; or S100A4) and fibroblast activation protein (FAP). However, due to their heterogeneity, not all markers can be identified on CAFs. In the present study, we identified all the CAF markers (α-SMA, S100A4 and FAP-α) on ihSTCs, but only α-SMA expression was identified in ihSTBMCs. However, the markers of mesenchymal cells, CD44 and CD105, were shown to be expressed on ihSTBMCs. Considering that ihSTBMCs are bone marrow-derived cells, this is reliable evidence to prove that tumor stroma fibroblasts originate from the bone marrow and are derived from MSCs.

The malignant potential of the two cell lines were then demonstrated *in vitro* and *in vivo*. The CCK-8 assay did not show any significant differences in the proliferation rates of ihSTCs and ihSTBMCs. However, the proliferation rates of the two cell lines were higher than those of SU3-RFP and NIH-3T3. Flow cytometric analysis of the cell cycle assay showed a marked increase in the number of ihSTCs and ihSTBMCs in the S phase, and this corresponded with the results of the CCK-8 assay. Anchorage-independent growth, which is generally recognized as a hallmark of oncogenic transformation, was examined. The colony-forming efficiency of ihSTCs and ihSTBMCs was higher than that of SU3-RFP and NIH-3T3 cells. The most useful evidence of malignant transformation is the tumorigenicity of the two cell lines *in vivo*. As shown in the present results, when ihSTCs and ihSTBMCs were injected into athymic nude mice, a 100% tumorigenesis rate (20/20) was observed with even as few as 1×10^6 cells (10/10). Furthermore, ihSTCs and ihSTBMCs showed stronger tumorigenicity than SU3-RFP cells in normal BALB/c mice. The morphological features of fusocellular sarcomas were evident in the H&E-stained sections. This finding is further evidence of its fibroblast-like phenotype.

Stromal cells within a tumor can be truly malignant and have been reported as early as 1981 (28), although it remains under investigation (30-34,49-51). Since it is almost impossible to distinguish between the tumor and stroma, *in vitro* studies involving direct or indirect co-culturing have been performed. Using the fluorescent tracing mouse model, we have demonstrated that stroma fibroblasts undergo malignant transformation, although whether this process occurred *in vitro* or *in vivo* remains to be determined, since the process of tumor growth *in vivo* occurs in approximately 30 days and the transplanted tumors were subcultured *in vitro* for approximately one week for sorting. As known, transplanted tumors in animals have a more complicated microenvironment. Additionally, the malignant transformation of MSCs and mouse embryonic fibroblasts was not observed with direct continual culture or co-culture with SU3-RFP via Transwell for over 2 months until apoptosis *in vitro* (data not shown). Therefore, we speculated that the process of malignant transformation was initiated *in vivo*. In addition, to prove that the viral vector containing the *RFP* gene transfected into SU3 cells did not exert any effect, SU3 cells that did not contain the *RFP* gene were transplanted into GFP nude mice, which yielded GFP-positive cells, similar to the results for SU3-RFP (data not shown).

The mechanisms involved in the transformation, however, are unclear and remain to be investigated. Goldenberg *et al*, one of the first investigators to study the malignant transformation of stromal cells, recently suggested that cell fusion of tumor and stromal cells is involved in malignancies (52). Furthermore, recent findings suggested that certain functional human genes may be involved in the malignant transformation of stromal cells (49,50). This view is also supported by other investigators (53-55). However, as shown above, two of the transformed cells cloned in the present study are of mouse origin, and only mouse chromosomes were observed. However, as reported by Pathak *et al* (53) and Jacobsen *et al* (54), it is possible that the tumor cells first fused with the stroma cells, led to loss of the tumor cell chromosomes. It has been argued that stimulation with cytokines such as IL-6, GM-CSF and IL-4 is a potential mechanism underlying the malignant transformation of stroma cells (32,56). However, all the experimental results are derived from *in vitro* co-culture systems, which may not completely represent the *in vivo* TME. Recent findings suggested that exosomes and the microRNAs secreted by breast cancer cells induce non-tumorigenic epithelial cells to form tumors (5). Microvesicles of cancer cells (gliomas) can contribute to the horizontal propagation of oncogenes, such as EGFRvIII, as previously reported (57), but whether these oncogenes can be passed on from cancer to stromal cells remains unknown.

In conclusion, in the present study, the bone marrow-derived tumor stromal cells ihSTCs and ihSTBMCs were found to be of murine MSC origin and showed a rapid growth rate, high cloning efficiency, high DNA content, expression of fibroblasts markers and high tumorigenicity. Taken together, these results demonstrate that the two cell lines are malignant transformed fibroblasts that originated from the bone marrow and were recruited by mesenchymal cells.

Acknowledgements

The present study was funded by the National Natural Scientific Foundation of China (nos. 81172400, 81272799, 81302196, 81302180 and 81472739).

References

1. Hanahan D and Weinberg RA: Hallmarks of cancer: The next generation. Cell 144: 646-674, 2011.
2. Tarin D: Role of the host stroma in cancer and its therapeutic significance. Cancer Metastasis Rev 32: 553-566, 2013.
3. Casazza A, Di Conza G, Wenes M, Finisguerra V, Deschoemaeker S and Mazzone M: Tumor stroma: A complexity dictated by the hypoxic tumor microenvironment. Oncogene 33: 1743-1754, 2014.
4. De Wever O, Demetter P, Mareel M and Bracke M: Stromal myofibroblasts are drivers of invasive cancer growth. Int J Cancer 123: 2229-2238, 2008.
5. Melo SA, Sugimoto H, O'Connell JT, Kato N, Villanueva A, Vidal A, Qiu L, Vitkin E, Perelman LT, Melo CA, *et al*: Cancer exosomes perform cell-independent microRNA biogenesis and promote tumorigenesis. Cancer Cell 26: 707-721, 2014.
6. Räsänen K and Vaheri A: Activation of fibroblasts in cancer stroma. Exp Cell Res 316: 2713-2722, 2010.
7. Worthley DL, Ruszkiewicz A, Davies R, Moore S, Nivison-Smith I, Bik To L, Browett P, Western R, Durrant S, So J, *et al*: Human gastrointestinal neoplasia-associated myofibroblasts can develop from BMDCS following allogeneic stem cell transplantation. Stem Cells 27: 1463-1468, 2009.
8. Quante M, Tu SP, Tomita H, Gonda T, Wang SS, Takashi S, Baik GH, Shibata W, Diprete B, Betz KS, *et al*: Bone marrow-derived myofibroblasts contribute to the mesenchymal stem cell niche and promote tumor growth. Cancer Cell 19: 257-272, 2011.
9. Bergfeld SA and DeClerck YA: Bone marrow-derived mesenchymal stem cells and the tumor microenvironment. Cancer Metastasis Rev 29: 249-261, 2010.
10. Hanahan D and Coussens LM: Accessories to the crime: Functions of cells recruited to the tumor microenvironment. Cancer Cell 21: 309-322, 2012.
11. Mishra PJ, Mishra PJ, Humeniuk R, Medina DJ, Alexe G, Mesirov JP, Ganesan S, Glod JW and Banerjee D: Carcinoma-associated fibroblast-like differentiation of human mesenchymal stem cells. Cancer Res 68: 4331-4339, 2008.
12. Kalluri R and Zeisberg M: Fibroblasts in cancer. Nat Rev Cancer 6: 392-401, 2006.
13. Ostman A and Augsten M: Cancer-associated fibroblasts and tumor growth - bystanders turning into key players. Curr Opin Genet Dev 19: 67-73, 2009.
14. Hayward SW, Wang Y, Cao M, Hom YK, Zhang B, Grossfeld GD, Sudilovsky D and Cunha GR: Malignant transformation in a nontumorigenic human prostatic epithelial cell line. Cancer Res 61: 8135-8142, 2001.
15. Olumi AF, Grossfeld GD, Hayward SW, Carroll PR, Tlsty TD and Cunha GR: Carcinoma-associated fibroblasts direct tumor progression of initiated human prostatic epithelium. Cancer Res 59: 5002-5011, 1999.
16. Bhowmick NA, Chytil A, Plieth D, Gorska AE, Dumont N, Shappell S, Washington MK, Neilson EG and Moses HL: TGF-beta signaling in fibroblasts modulates the oncogenic potential of adjacent epithelia. Science 303: 848-851, 2004.
17. Kuperwasser C, Chavarria T, Wu M, Magrane G, Gray JW, Carey L, Richardson A and Weinberg RA: Reconstruction of functionally normal and malignant human breast tissues in mice. Proc Natl Acad Sci USA 101: 4966-4971, 2004.

18. Bhowmick NA, Neilson EG and Moses HL: Stromal fibroblasts in cancer initiation and progression. Nature 432: 332-337, 2004.
19. Russell PJ, Bennett S and Stricker P: Growth factor involvement in progression of prostate cancer. Clin Chem 44: 705-723, 1998.
20. Tlsty TD and Hein PW: Know thy neighbor: Stromal cells can contribute oncogenic signals. Curr Opin Genet Dev 11: 54-59, 2001.
21. Hu M, Yao J, Cai L, Bachman KE, van den Brûle F, Velculescu V and Polyak K: Distinct epigenetic changes in the stromal cells of breast cancers. Nat Genet 37: 899-905, 2005.
22. Paterson RF, Ulbright TM, MacLennan GT, Zhang S, Pan CX, Sweeney CJ, Moore CR, Foster RS, Koch MO, Eble JN, *et al*: Molecular genetic alterations in the laser-capture-microdissected stroma adjacent to bladder carcinoma. Cancer 98: 1830-1836, 2003.
23. Moinfar F, Man YG, Arnould L, Bratthauer GL, Ratschek M and Tavassoli FA: Concurrent and independent genetic alterations in the stromal and epithelial cells of mammary carcinoma: Implications for tumorigenesis. Cancer Res 60: 2562-2566, 2000.
24. Houghton J, Li H, Fan X, Liu Y, Liu JH, Rao VP, Poutahidis T, Taylor CL, Jackson EA, Hewes C, *et al*: Mutations in bone marrow-derived stromal stem cells unmask latent malignancy. Stem Cells Dev 19: 1153-1166, 2010.
25. Bernardo ME, Zaffaroni N, Novara F, Cometa AM, Avanzini MA, Moretta A, Montagna D, Maccario R, Villa R, Daidone MG, *et al*: Human bone marrow derived mesenchymal stem cells do not undergo transformation after long-term in vitro culture and do not exhibit telomere maintenance mechanisms. Cancer Res 67: 9142-9149, 2007.
26. Gou S, Wang C, Liu T, Wu H, Xiong J, Zhou F and Zhao G: Spontaneous differentiation of murine bone marrow-derived mesenchymal stem cells into adipocytes without malignant transformation after long-term culture. Cells Tissues Organs 191: 185-192, 2010.
27. Luetzkendorf J, Nerger K, Hering J, Moegel A, Hoffmann K, Hoefers C, Mueller-Tidow C and Mueller LP: Cryopreservation does not alter main characteristics of Good Manufacturing Process-grade human multipotent mesenchymal stromal cells including immunomodulating potential and lack of malignant transformation. Cytotherapy 17: 186-198, 2015.
28. Goldenberg DM and Pavia RA: Malignant potential of murine stromal cells after transplantation of human tumors into nude mice. Science 212: 65-67, 1981.
29. Sparrow S, Jones M, Billington S and Stace B: The in vivo malignant transformation of mouse fibroblasts in the presence of human tumour xenografts. Br J Cancer 53: 793-797, 1986.
30. Røsland GV, Svendsen A, Torsvik A, Sobala E, McCormack E, Immervoll H, Mysliwietz J, Tonn JC, Goldbrunner R, Lønning PE, *et al*: Long-term cultures of bone marrow-derived human mesenchymal stem cells frequently undergo spontaneous malignant transformation. Cancer Res 69: 5331-5339, 2009.
31. Liu J, Zhang Y, Bai L, Cui X and Zhu J: Rat bone marrow mesenchymal stem cells undergo malignant transformation via indirect co-cultured with tumour cells. Cell Biochem Funct 30: 650-656, 2012.
32. Cui X, Liu J, Bai L, Tian J and Zhu J: Interleukin-6 induces malignant transformation of rat mesenchymal stem cells in association with enhanced signaling of signal transducer and activator of transcription 3. Cancer Sci 105: 64-71, 2014.
33. Serrano-Heras G, Domínguez-Berzosa C, Collantes E, Guadalajara H, García-Olmo D and García-Olmo DC: NIH-3T3 fibroblasts cultured with plasma from colorectal cancer patients generate poorly differentiated carcinomas in mice. Cancer Lett 316: 85-90, 2012.
34. Yu F, Hsieh WS, Petersson F, Yang H, Li Y, Li C, Low SW, Liu J, Yan Y, Wang DY, *et al*: Malignant cells derived from 3T3 fibroblast feeder layer in cell culture for nasopharyngeal carcinoma. Exp Cell Res 322: 193-201, 2014.
35. Yang M, Reynoso J, Jiang P, Li L, Moossa AR and Hoffman RM: Transgenic nude mouse with ubiquitous green fluorescent protein expression as a host for human tumors. Cancer Res 64: 8651-8656, 2004.
36. Dong J, Dai XL, Lu ZH, Fei XF, Chen H, Zhang QB, Zhao YD, Wang ZM, Wang AD, Lan Q, *et al*: Incubation and application of transgenic green fluorescent nude mice in visualization studies on glioma tissue remodeling. Chin Med J 125: 4349-4354, 2012.
37. Iyer S, Arindkar S, Mishra A, Manglani K, Kumar JM, Majumdar SS, Upadhyay P and Nagarajan P: Development and evaluation of transgenic nude mice expressing ubiquitous green fluorescent protein. Mol Imaging Biol 17: 471-478, 2015.
38. Ricard C and Debarbieux FC: Six-color intravital two-photon imaging of brain tumors and their dynamic microenvironment. Front Cell Neurosci 8: 57, 2014.
39. Suetsugu A, Katz M, Fleming J, Truty M, Thomas R, Moriwaki H, Bouvet M, Saji S and Hoffman RM: Multi-color palette of fluorescent proteins for imaging the tumor microenvironment of orthotopic tumorgraft mouse models of clinical pancreatic cancer specimens. J Cell Biochem 113: 2290-2295, 2012.
40. Duda DG, Fukumura D, Munn LL, Booth MF, Brown EB, Huang P, Seed B and Jain RK: Differential transplantability of tumor-associated stromal cells. Cancer Res 64: 5920-5924, 2004.
41. Wang A, Dai X, Cui B, Fei X, Chen Y, Zhang J, Zhang Q, Zhao Y, Wang Z, Chen H, *et al*: Experimental research of host macrophage canceration induced by glioma stem progenitor cells. Mol Med Rep 11: 2435-2442, 2015.
42. Huang Q, Zhang QB, Dong J, Wu YY, Shen YT, Zhao YD, Zhu YD, Diao Y, Wang AD and Lan Q: Glioma stem cells are more aggressive in recurrent tumors with malignant progression than in the primary tumor, and both can be maintained long-term in vitro. BMC Cancer 8: 304, 2008.
43. Wan Y, Fei XF, Wang ZM, Jiang DY, Chen HC, Yang J, Shi L and Huang Q: Expression of miR-125b in the new, highly invasive glioma stem cell and progenitor cell line SU3. Chin J Cancer 31: 207-214, 2012.
44. Okabe M, Ikawa M, Kominami K, Nakanishi T and Nishimune Y: 'Green mice' as a source of ubiquitous green cells. FEBS Lett 407: 313-319, 1997.
45. Seabright M: A rapid banding technique for human chromosomes. Lancet 2: 971-972, 1971.
46. Bouvet M and Hoffman RM: Tumor imaging technologies in mouse models. Methods Mol Biol 1267: 321-348, 2015.
47. Suetsugu A, Osawa Y, Nagaki M, Saji S, Moriwaki H, Bouvet M and Hoffman RM: Imaging the recruitment of cancer-associated fibroblasts by liver-metastatic colon cancer. J Cell Biochem 112: 949-953, 2011.
48. Zhu L, Cheng X, Ding Y, Shi J, Jin H, Wang H, Wu Y, Ye J, Lu Y, Wang TC, *et al*: Bone marrow-derived myofibroblasts promote colon tumorigenesis through the IL-6/JAK2/STAT3 pathway. Cancer Lett 343: 80-89, 2014.
49. Goldenberg DM, Rooney RJ, Loo M, Liu D and Chang CH: In-vivo fusion of human cancer and hamster stromal cells permanently transduces and transcribes human DNA. PLoS One 9: e107927, 2014.
50. Goldenberg DM, Gold DV, Loo M, Liu D, Chang CH and Jaffe ES: Horizontal transmission of malignancy: In-vivo fusion of human lymphomas with hamster stroma produces tumors retaining human genes and lymphoid pathology. PLoS One 8: e55324, 2013.
51. He X, Li B, Shao Y, Zhao N, Hsu Y, Zhang Z and Zhu L: Cell fusion between gastric epithelial cells and mesenchymal stem cells results in epithelial-to-mesenchymal transition and malignant transformation. BMC Cancer 15: 24, 2015.
52. Goldenberg DM, Zagzag D, Heselmeyer-Haddad KM, Berroa Garcia LY, Ried T, Loo M, Chang CH and Gold DV: Horizontal transmission and retention of malignancy, as well as functional human genes, after spontaneous fusion of human glioblastoma and hamster host cells in vivo. Int J Cancer 131: 49-58, 2012.
53. Pathak S, Nemeth MA, Multani AS, Thalmann GN, von Eschenbach AC and Chung LW: Can cancer cells transform normal host cells into malignant cells? Br J Cancer 76: 1134-1138, 1997.
54. Jacobsen BM, Harrell JC, Jedlicka P, Borges VF, Varella-Garcia M and Horwitz KB: Spontaneous fusion with, and transformation of mouse stroma by, malignant human breast cancer epithelium. Cancer Res 66: 8274-8279, 2006.
55. Rappa G, Mercapide J and Lorico A: Spontaneous formation of tumorigenic hybrids between breast cancer and multipotent stromal cells is a source of tumor heterogeneity. Am J Pathol 180: 2504-2515, 2012.
56. Zhou XG, Yang Y, Yang JS, Zhou J, Fang TL, Dai WD and Chen ZR: Granulocyte-macrophage colony-stimulating factor and interleukin 4 induce the malignant transformation of the bone marrow-derived human adult mesenchymal stem cells. Chin Med J 124: 729-733, 2011.
57. Al-Nedawi K, Meehan B, Micallef J, Lhotak V, May L, Guha A and Rak J: Intercellular transfer of the oncogenic receptor EGFRvIII by microvesicles derived from tumour cells. Nat Cell Biol 10: 619-624, 2008.